Military Technical College
Kobry El-Kobbah,
Cairo, Egypt.

13th International Conference on Applied Mechanics and Mechanical Engineering.

SILVER TOUGHENED ALUMINA CUTTING TOOL INSERTS: PERFORMANCE EVALUATION USING DYNAMIC COMPONENTS OF CUTTING FORCE SPECTRA

DUTTA* A. K., GUHA** A. and RAY*** K. K.

ABSTRACT

Cutting tool inserts have been fabricated using alumina with different amounts of silver by conventional powder metallurgical route. The machining performance of these composite inserts vis-à-vis that of commercial zirconia toughened alumina inserts have been evaluated by dry turning operations on steel bars under a wide range of cutting parameters. The experiments consisted of measurement and examinations of the static and the dynamic components of the cutting force spectra, flank wear of the tool, surface roughness on the work piece, and chip morphology. Analyses of the fluctuations in the dynamic force spectra using a new approach based on a quasi-fractal model have been used to reveal the potential of different tool materials with respect to their cutting performance. Examinations and pertinent discussion of the operative wear mechanisms during machining by the developed composites vis-à-vis their structure-property relations are some essential supplements of this investigation.

KEY WORDS

Alumina-silver Composite, Toughness, Machining Performance, Flank wear, Dynamic force.

* Professor, Dept. of Mechanical Engineering, Bengal Engineering and Science University, Howrah, India.
** Lecturer, Mechanical Engineering, Bengal Engineering and Science University, Howrah, India.
*** Professor, Dept of Metallurgical & Materials Engineering, Indian Institute of Technology, Kharagpur, India.

INTRODUCTION

One of the perpetual challenges in the metal cutting discipline is to develop newer cutting tool inserts with improved combinations of chemical stability, abrasion resistance, hardness, toughness and thermal conductivity. This has led to the emergence of a variety of ceramic matrix composites in which undoubtedly the alumina matrix composites (AMC) represent the most distinguished class since these materials inherently possess excellent chemical stability, wear resistance and hot hardness; but these are usually coupled with limited fracture toughness and thermal shock resistance. In order to overcome the limitation of low fracture toughness, advanced alumina ceramics have been developed with the addition of zirconia [1,2], titanium carbide [3,4] or silicon carbide [5,6]. Toughening of alumina can also be done with the addition of metallic particles [7-11], but the potential of such metal toughened alumina composites has not been fully explored. Some recent reports [12-16] related to the characteristics of silver toughened alumina indicate that this material can be used for cutting tool applications.

The process of development of newer materials amenable for fabricating cutting tool inserts usually demands a two-fold approach for in-depth investigation. The structure-property co-relations need to be gauged from the view point of materials technology while the assessment of machining performance of the inserts, made from the developed materials, need to be examined using the approach of mechanical science. In the latter category usually tool life estimation is considered as the best performance index. But it does not provide sufficient information related to the on-line behavior of the cutting tool. Over the last decade, several attempts [17-21] have been made to achieve solution to this problem without any significant success. A pioneering attempt is made in this report to derive a parameter for on-line tool monitoring of cutting performance employing the concept of fractal geometry to the analysis of dynamic force spectrum generated from tool-work interactions. This parameter, machining index, is also considered to grade the performance of the various cutting tool inserts. The major aim of this report is to grade the performance of a series of developed silver toughened alumina composites using the proposed quasi-fractal parameter. The process of making the alumina-silver composites and the characterizations of their structure and pertinent properties are essential supplements to the primary theme of the work.

EXPERIMENTAL

The alumina–silver composites were prepared from powder mixtures of commercial α-alumina and varying amounts of silver oxide. The details of the processing route have been reported earlier [14,15]. In brief, a powder blend of α-Al_2O_3 (doped with 0.5 wt.% MgO) and Ag_2O was milled for 8 h in an alcohol medium and the blended powder was crushed with a few drops of polyvinyl alcohol (PVA) solution as binder, and was sieved. The powder mixture was then subjected to compaction to produce square shaped green pellets which were fired at 500^oC for 5 h to burn off the PVA binder. The fired pellets were then pre-sintered at 1100^oC for 2 h followed by final sintering at 1550^oC for 2 h under atmospheric conditions. An identical process route was followed to prepare composites by altering Ag_2O content as 5, 10 and 15 wt.% and monolithic alumina doped with MgO. Unlike the composites, the monolithic alumina specimens were sintered at 1600^oC for 2 h. The bulk density, open porosity and the relative density of

the different types of pellets were determined using the boiling water method [22] following Archimedes' principle.

Phase identification in the prepared samples was made by X-ray diffraction analysis using a Philips PW1729 X-ray diffractometer. The microstructures of metallographiclly polished samples were examined using a light microscope and a Jeol JSM 5800 scanning electron microscope. Representative photographs of the composites were taken during these examinations. The volume fraction of silver particles in the alumina–silver composites was ascertained by standard point counting technique. The grain size of the alumina matrix was determined by the linear intercept method from SEM photographs of the fractured surfaces.

The hardness values of the prepared composites were measured using a Knoop indentor with the help of a LECO DM400 microhardness tester. Fracture toughness values of the developed materials were determined by indentation method using the formula suggested by Lankford [23]. The indentation cracks were generated using a Vickers indenter at an indentation load of 98 N. Cutting tool inserts, conforming to ISO specification SNGN 120408, were prepared from the sintered pellets by following the same grinding procedure used for making specimens for microstructural studies and mechanical tests. Nose radius of 0.8mm was carefully provided on each corner of the inserts using a diamond file of 20–40 μm grit size with intermittent examination of the nose through a Olympus SZ-PT stereomicroscope fitted with a graduated eyepiece. Land width of 0.1mm at an angle 20^{o} was provided on each cutting edge by holding the specimen in a fixture and polishing on 1000 μm grit size SiC paper. After beveling, the sharp edges were rounded off (to a radius of 20–30 μm) by light honing with diamond paste of 3 μm size on a Buehler Ecomet 3 lapping machine. The machining performance of these inserts was examined by plain dry turning of C45 steel (C-0.47%, 200 BHN) in an 11kW rigid HMT NH22 centre lathe. Turning tests were carried out for a wide range of cutting velocity (150–400 m/min), feed (0.12–0.24 mm/rev.) and depth of cut (1.5 and 2.0 mm). During turning, the tangential (*Pz*) and the axial (*Px*) components of cutting force were measured using a Kistler 9257B piezoelectric turning dynamometer.

Tool inserts were withdrawn at regular intervals from the turning operation and the magnitude of the average flank wear at each interruption was measured by an optical microscope. The pattern and the degree of degradation of the turning inserts, used for machining, were examined using a scanning electron microscope. The chips were collected during turning operation under different combinations of cutting parameters for subsequent examination.

RESULTS AND DISCUSSION

The results of this investigation can be broadly categorized under three groups related to: (a) microstructure, (b) physical and mechanical properties and (c) machining performance of the prepared inserts. The salient features of these results and their pertinent discussions are presented below in different sub-sections.

Microstructural Examinations

The prepared monolithic alumina and the different alumina–silver composites are henceforth referred to as Ag-0, Ag-5, Ag-10 and Ag-15 in accordance with the wt.% of Ag_2O in the initial powder mix for convenience of subsequent discussions. The selected weight percentages of Ag_2O powder are expected to theoretically yield nearly 2–6 vol.% of Ag in the fabricated composites. The gray colored Al_2O_3–Ag_2O green compacts turned white on sintering. During sintering Ag_2O gets decomposed to metallic Ag leading to the formation of Al_2O_3–Ag system. At temperatures above 1000°C, Ag starts evaporating from the surfaces of the alumina–silver specimens. The alumina particles on the surfaces while getting sintered make a barrier to prevent further escape of Ag by evaporation. This phenomenon leads to a silver depleted surface layer and a silver-rich central region in the sintered pellets. Identification of phases at surface layers of different depth by X-ray diffraction analyses illustrated the existence of a graded microstructure in the fabricated composites; the amount of Ag is observed to increase from the surface towards the central region of a specimen of the alumina–silver composites. The almost silver-free white surface layer is called as the rim while the silver-rich gray central region is called as the core of the fabricated pellets. A typical rim-core type composite is illustrated in Fig. 1. The rim thicknesses of the different composites were measured and their values are shown in Table 1. A typical fractograph of an alumina–silver composite, shown in Fig. 2, illustrates the grain size of the alumina matrix. The average grain size of the matrix for all the composites can be designated as 1.4±0.2μm. Microscopic examinations indicated uniform distribution of silver particles in the alumina matrix (Fig. 3). The measured volume fractions of silver in the alumina–silver composites were approximately 10–15% lower than the theoretical estimates. The measured lower values compared to the theoretical estimates of the amount of silver in the fabricated composites are attributed to the loss of silver by evaporation during sintering.

Physical and Mechanical Properties

The relative densities of the fabricated materials are shown in Table 1. The relative density of Ag-10 is found to be the highest amongst the developed composites. Hardness values (Hk) of the developed materials, have been determined using Knoop indenter at different loads, are found to exhibit indentation size effect. In order to compare the hardness values of the developed materials, the true hardness (H_0) values were estimated for the developed materials using the following expression [14]:

$$d = \left(\frac{14229}{H_O}\right)^{\frac{1}{2}} P^{\frac{1}{2}} - d_e \qquad (1)$$

where d is the measured diagonal, P is the indentation load and d_e is the amount of relaxation in indentation diagonal. The procedure for estimating H_0 has been described elsewhere [14]. The true hardness values for the developed composites are given in Table 2. The results indicate that H_0 is generally lower than that of the conventional H_k values. The fracture toughness values of the developed materials have been determined by indentation technique and the estimated toughness values are given in Table 1. The results in Table 1 indicate that higher amount of silver in the developed composites increases their fracture toughness but decreases their hardness. The increase in fracture toughness (based on H_0 values) from Ag-0 to Ag-15 samples is

nearly 160%, but the associated degradation of hardness (H_0) for similar materials is only about 35%. The higher fracture toughness of silver containing composites has been attributed to the mechanisms of ductile particle stretching and crack deflection.

Machining Performance Tests

On chip morphology

The type of chips produced during machining operations has significant effect on both the generated surface finish and the rate of tool wear. Thus, analysis of chip morphology is important for assessing any machining performance test. The developed tool inserts produced thin, long and nearly uniform chips at low feeds of 0.12 and 0.16 mm/rev. At higher feeds the chips were observed to be thick and closely curled, which broke into almost half-turn pieces by striking against the tool flank. Only in the case of monolithic alumina (Ag-0) inserts, the chips gradually became constrained and non-uniform even at lower feed until V_c was raised to 350 m/min. This phenomenon is attributed to the lack of resistance to micro-chipping and crushing of the fresh edges of this insert. Among the alumina–silver inserts, Ag-10 having silver content of 3.38 vol.% has been found to be the most satisfactory one with respect to cutting edge stability and chip formation.

On cutting force

Knowledge about the cutting forces in machining assists in designing both the machine tool and the cutting tool, and in achieving optimized cutting conditions. In this investigation the magnitudes of the tangential (*Pz*) and the axial (*Px*) components of the cutting forces have been examined. Amongst the cutting force components, *Pz* is the most significant one because it is largest in magnitude and governs the power consumption in the process of cutting. Next important is the axial component (*Px*) because it gets considerably influenced by the nature and the extent of interaction of the chip–tool interface. The third component i.e. transverse force (*Py*) is much less significant because its magnitude is considerably low for wide cutting edge angle.

Figure 4 represents typical variations of *Pz* and *Px* with cutting velocity at constant feed (S_0) and depth of cut (t). The magnitudes of *Pz* and *Px* are found to decrease with increase in cutting velocity. Detail investigation also indicates that the magnitudes of *Pz* and *Px* increase substantially with increase in feed for all the inserts. A closer examination on the nature of the variation in *Pz* and *Px*, reveals that the performances of Ag-10 inserts closely resemble that of ZTA inserts for the investigated range of cutting parameters. The results obtained related to cutting forces in all the experiments also indicate that Ag-10 inserts exhibit the best performance amongst the developed tools with respect to the stability of the cutting edges and chip–tool interactions.

On tool wear

All the developed tools as well as the ZTA insert were subjected to initial wear test at high cutting velocity (400 m/min), feed (0.24 mm/rev.) and depth of cut (1.5 mm) for duration of 4 min. While machining steel bar by the different tools, each tool was withdrawn at regular intervals and the nature and extent of their wear and cutting edge conditions were examined under SEM and optical microscope. It was found that the cutting edge conditions and wear rate of the Ag-10 inserts were more or less stable as that of the ZTA insert after their break-in wear stage. The nature of growth of the average flank wear (V_B) measured with the progress of machining up to 4 min at high

V_C and S_0 is shown in Fig. 5. The results in Fig. 5 depict that the ZTA and the Ag-10 inserts attain much less flank wear compared to the other inserts. The Ag-0, Ag-5 and Ag-15 inserts which were found to work quite satisfactorily for the first few seconds of machining with respect to chip formation and cutting forces, were found to exhibit considerable break-in wear within about 1 min. This may be attributed to the fact that initially the cutting edges of these inserts were fresh but with the progress of time, lack of either adequate toughness (in Ag-0 and Ag-5 inserts) or hardness (in Ag-15) contributed to rapid break-in wear. However, after the break-in wear stage Ag-0, Ag-5 and Ag-15 inserts also showed steady growth in flank wear.

On the dynamic components of cutting force spectra

The magnitude and the pattern of the cutting force components change with machining time and depend on tool wear and the interaction between the cutting tool and the work material under given speed, feed and depth of cut. The spectrum of each of these force components consists of a static and a dynamic component. The static part is conventionally defined as the average cutting force whereas the dynamic part implies the deviation of force value at any instance of time from the static value (Fig.6). The fluctuations in the cutting force (Fig.6) originate from the (i) variable speed of the tool relative to the work-piece, (ii) the influence of cutting action of the flat cutting edge at the tool point, (iii) the variable depth of cut and (iv) variable rake condition. Such fluctuations are contended to be related to tool wear and several attempts have been directed to characterize the pattern of dynamic force components using spectral analysis [17,18]), pattern recognition [19], fuzzy logic [20]) or neural network analysis [21] in order to relate the parameters derived from these analyses to tool wear behaviour. But these investigations have not been able to provide any specific guideline to characterize the relative cutting performance of different tool materials.

The dynamic force spectrum can be considered as a signature of tool-work interaction. Such a signature originates from superposition of several noises from depth of cut, inhomogeneity of work material, built-up-edge formation, chipping and wear of tool etc. on a regular pattern of force variation during the formation and breaking of chips during machining. One can consider an idealized force variation during machining (Fig.7.a) and may assume different types of noise (Fig.7b, c and d) resulting from different sources. Superimposition of these noises on the assumed idealized force pattern would change the resultant signal (Fig.7e, f and g). But it is difficult to separate out the individual sources of the noises to understand the physical nature of tool work interaction. It is also to be borne in mind that the resultant signal bears the characteristics of the tool material for a fixed machine-fixture-tool-work combination.

It is hypothesized in this investigation that the total length of dynamic force component signal per unit time is a material characteristic representing the behaviour of a tool against a work material. This parameter for the axial (P_X) and the tangential (P_Z) components for the dynamic force was estimated for the different tools investigated in this study, and their estimated magnitudes are designated as M_X and M_Z. The variations in the suggested parameter against cutting velocity and feed are shown in Fig.8. It is obvious that the magnitudes of these estimated parameters are, in general, minimum for Ag-10 and ZTA inserts indicating these to be the best tool materials amongst the examined ones. This is based on the consideration that M_X and M_Z are some quasi-fractal parameters as discussed below.

The concept of fractal geometry is well established [24] and the fractal dimension (D) of an irregular curve can be conveniently achieved by the Mandelbrot-Richardson [24] expression which is based on estimating the true (L_t) and projected length (L_o) of a curve with different divider spans (η). The relation between these parameters indicates (Ray and Mondal 1992).

$$\ln (L_t/L_o) = - (D-1) \ln \eta$$

Thus for a dynamic force spectrum if its true length is estimated per unit time by identical approaches, one fixes the L_o and the η values. Hence the measured length M_X or M_Z are reflections of the value L_t which is naturally related to D. Higher magnitudes of M_X or M_Z indicate higher D or higher disturbances in the force generated during the cutting process and vice-versa. Thus M_X and M_Z are some quasi-fractal parameter to delineate the potential of cutting tool materials. The results in Fig.8 thus unambiguously lead to infer that Ag-10 and ZTA tools have resulted relatively better performance in turning operation. These performance-indices are well supported by the observations made during the study of chip morphology, static force behaviour and tool wear in this investigation. The relatively better performance of Ag-10 insert amongst all the developed ones is attributed to its best possible combination of higher hardness and toughness values (Table 1).

CONCLUSIONS

The following major conclusions can be derived from the results and the analyses presented in this study

(1) Addition of silver to alumina leads to structurally graded potential material for advanced ceramic cutting tool for machining.

(2) The cutting performance of the fabricated Ag-10 insert is comparable to that of industrially made ZTA insert.

(3) A new machining index to evaluate relative performance based on work-tool interaction has been proposed on the basis of quasi-fractal analysis of dynamic force patterns.

(4) The proposed machining index permits grading of tool materials with respect to their interactions with the work piece. The suggested gradation is in agreement with the one expected from the relative combination of hardness and toughness properties of these materials.

ACKNOWLEDGEMENT

The authors gratefully acknowledge the All India Council for Technical Education, Government of India for partly sponsoring this work under the grant no.8002/RID/NPRO/RPS-46/2003-04. The authors also thankfully acknowledge the critical discussion on the topic provided by Professor A. B. Chattopadhya of Mechanical Engineering Department of the Indian Institute of Technology, Kharagpur.

REFERENCES

[1] Garvie, R.C., "Microstructure and performance of an alumina–zirconia tool Bit", J. Mater. Sci., Vol. 3, pp 315–318, (1984).

[2] Mondal, B., Chattopadhyay, A.B., Virkar, A. and Paul, A., "Development and performance of zirconia–toughened alumina ceramic tools", Wear, Vol. 156, pp 365–383, (1992).

[3] Barry, J. and Byrne, G., "Cutting tool wear in the machining of hardened steels, Part I: Alumina/TiC cutting tool wear", Wear, Vol.247, pp139–151, (2001).

[4] Gruss, W. W. and Friederich, K. M., "Aluminum oxide/titanium carbide composite tools" in: E.D. Whitney (Ed.), Ceramic Cutting Tools – Materials, Development and Performance, Noyes Publ., NJ, USA, pp 63–85, (1994).

[5] Wei, G.C. and Becher, P.F., "Development of SiC–whisker–reinforced ceramics", Am. Ceram. Soc. Bull., Vol. 64 298–304(1985) .

[6] Casto, S. L., Valvo, E. L., Lucchini, E. and Ruisi V. F., "Wear rates and wear mechanisms of alumina-based tools cutting steel at low cutting speed",Wear, Vol. 208, pp 67–72,(1997) .

[7] Gu, X. and Hand, R.J., "The production of reinforced aluminium/alumina bodies by directed metal oxidation", J. Eur. Ceram. Soc., Vol. 15, pp 823–831, (1995).

[8] Sun, X. and Yeomans, J.A., "Microstructure and fracture toughness of nickel particle toughened alumina matrix composites", J. Mater. Sci., Vol. 31, pp 875–880, (1996).

[9] Anappara, A. A., Ghosh, S. K., Warrier, P. R. S., Warrier, K. G. K. and Wunderlich, W., "Impendence spectral studies of sol–gel alumina–silver nanocomposites", Acta Mater., Vol. 51, pp 3511–3519, (2003) .

[10] Wang, J., Ponton, C.B. and Marquis, P.M., "Silver–toughened alumina ceramic", Br. Ceram. Trans., Vol. 92, pp 67–74, (1993).

[11] Chou, W.B. and Tuan, W.H., 'Toughening and strengthening of alumina with silver inclusions", J. Eur. Ceram. Soc., Vol. 15, pp 291–295, (1995).

[12] Dutta, A. K., Chattopadhya, A. B. and Ray, K. K., "A study on alumina–5 vol.% silver composite as cutting tool insert", J. Mater. Sci. Lett., Vol.19, pp1501–1503, (2000).

[13] Dutta, A. K., Chattopadhya, A. B. and Ray, K. K., "An examination of alumina–1.6 vol.% silver composite as cutting tool insert", J. Mater. Sci. Lett., Vol. 20, pp917–919, (2001).

[14] Dutta, A. K., Narasaiah, N., Chattopadhya, A. B. and Ray, K. K., "The load dependence of hardness in alumina–silver composites", Ceram. Int., Vol. 27, pp 407–413, (2001).

[15] Dutta, A. K., Narasaiah, N., Chattopadhya, A. B. and Ray, K. K., "Influence of microstructure on wear resistance parameter of ceramic cutting tools", Mater. Manuf. Process, Vol. 17, pp 651–670, (2002).

[16] Dutta, A. K., Chattopadhya, A. B. and Ray, K. K., "Progressive flank wear and machining performance of silver toughened alumina cutting tool inserts", Wear, Vol. 261, pp 885 -895, (2006).

[17] Lee, L. C., Lee, K. S. and Gan, C. S., "On the correlation between dynamic cutting force and tool wear", *Int. J. Mach. Tools Manfact.*, Vol. 29, pp295-303, (1989).

[18] Teo, S. C., Lee, K. S. and Lee, L. C., "A study of the consistency of tool wear characteristics and the criteria for the onset of tool failure", *J. Materials Processing Technology*, Vol.37, pp.629-637 (1993).

[19] Emel, E. and Kannatey-Asibu, E., "Tool failure monitoring in turning by pattern recognition analysis of AE signals", *Trans. ASME, J. Eng. Ind.*, Vol.110, pp 137-145, (1988).

[20] Li, P. G. and Wu, S. M., "Monitoring drilling wear states by a fuzzy pattern recognition technique", *Trans. ASME, J. Eng. Ind.*, Vol.110, pp 297-300, (1988).

[21] Rangawala, S. and Dornfeld, D., "Sensor integration using neural networks for intelligent tool condition monitoring", *Trans. ASME, J. Eng. Ind.*, Vol.112, pp 219-298, (1990).

[22] Kingery, W.D., Bowen, H.K. and. Uhlmann, D.R , Introduction to Ceramics, 2nd ed., John Wiley & Sons, New York, pp 530–532, (1976).

[23] Lankford, J., "Indentation microfracture in the Palmqvist crack regime: implications for fracture toughness evaluation by the indentation method", J. Mater. Sci. Lett. Vol.1, pp 493–495, (1982) .

[24] Mandelbrot, B B, Passoja, D E, Pullay, A J, "Fractal character of fracture surfaces of metals",*Nature, Lond*, Vol. 308, p 721-722,(1984),

[25] Ray, K. K. and Mondal, G., "Study of correlation between fractal dimension and impact energy in a high strength low alloy steel", *Acta. Metall. Mater.*, Vol.40, pp 463-469, (1992).

Table and figures:

Table 1: Microstructural features and some properties of the investigated tool inserts

Matl. code	Average silver content [vol.%]	Average grain size [μm]	Relative density [%]	Rim Thick-ness [μm]	Hardness [GPa]		IFT [MPam$^{1/2}$]
					H_K	H_O	
Ag-0	-	1.4 ± 0.2	98.06	0	25.46	16.15	3.38
Ag-5	1.6		96.19	472	19.89	13.3	5.4
Ag-10	3.76		97.96	348	16.49	12.97	7.3
Ag-15	5.01		94.20	295	13.46	10.04	8.8

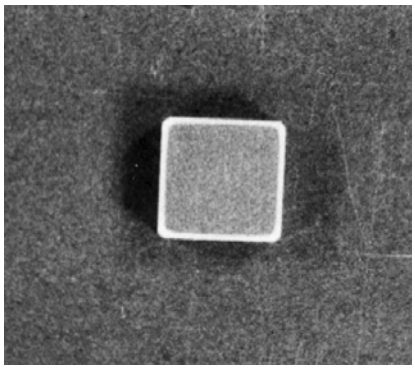

Fig. 1. A typical rim and core macrostructure of alumina–silver composite pellet

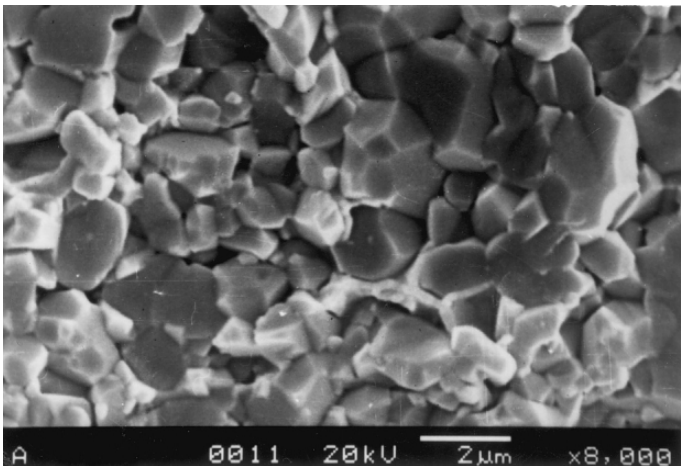

Fig. 2. A typical fractograph of alumina–silver composite used for grain size measurement.

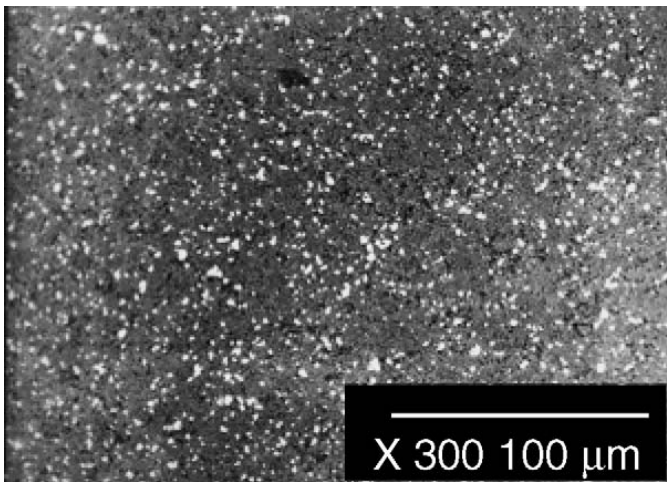

Fig.3. Typical distribution of silver particles in an alumina–silver composite

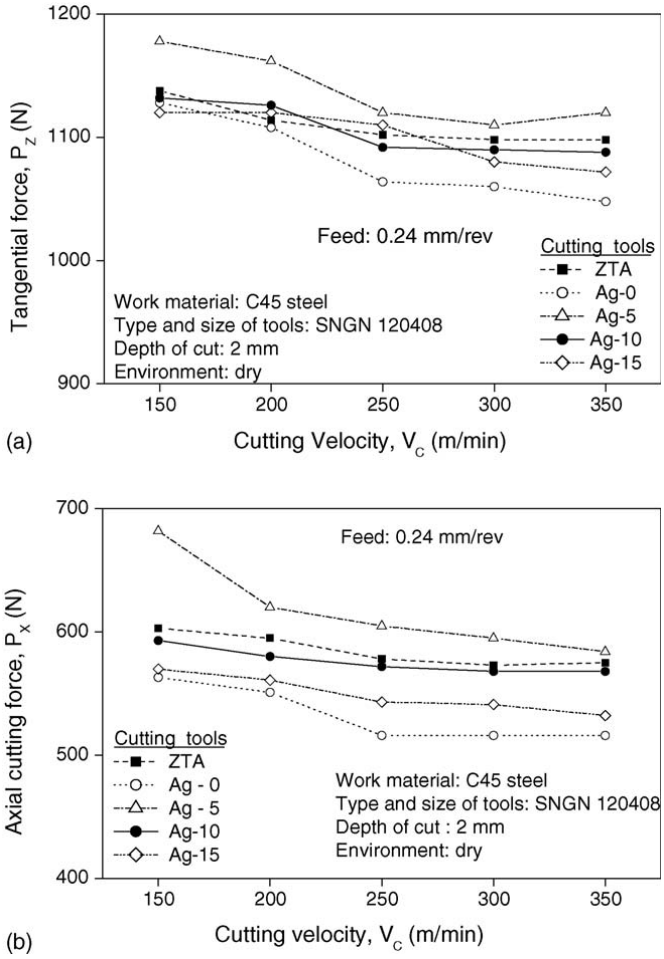

Fig. 4. Variation of (a) tangential and (b) axial components of force with cutting velocity at constant feed and depth of cut for all inserts.

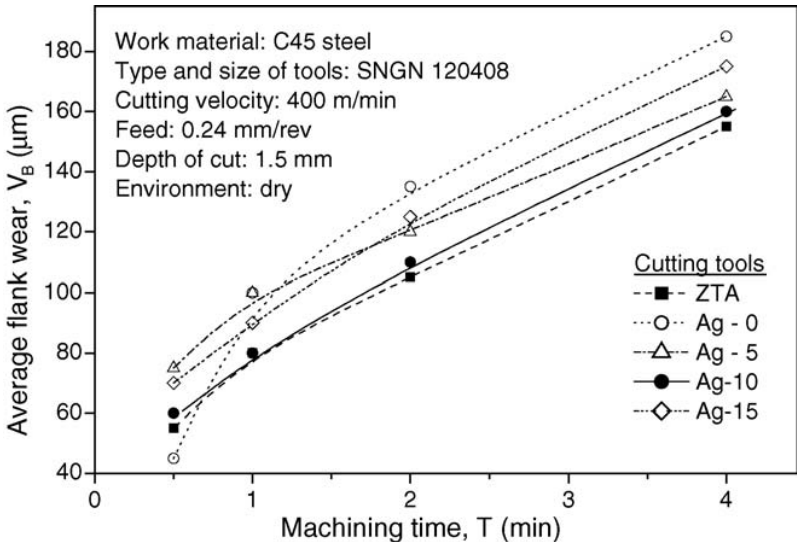

Fig.5. Progressive flank wear with machining time up to 4 min.

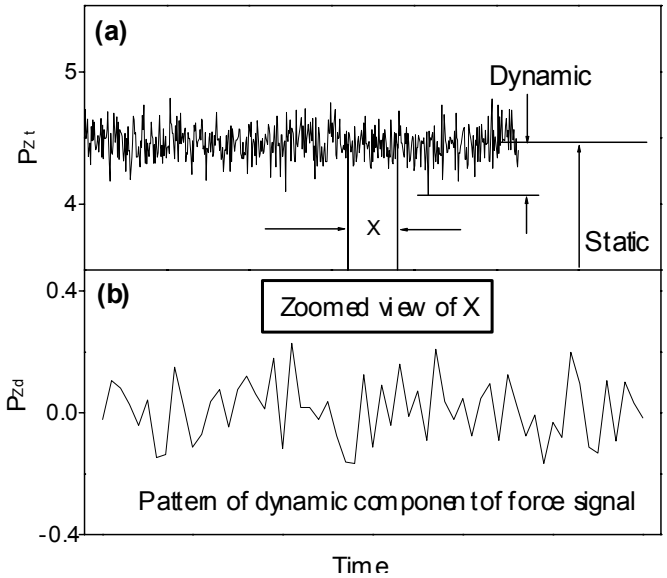

Fig.6. A typical recorded force spectrum.
(P_{Zt} and P_{zd} are total and dynamic forces respectively)

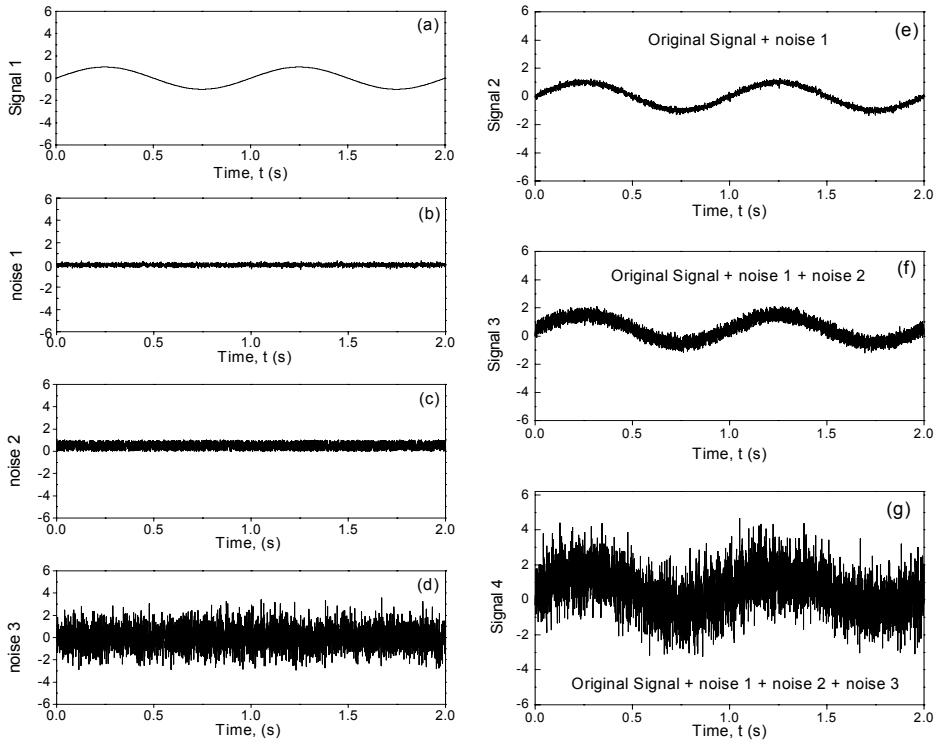

Fig.7. (a) Original signal, (b,c,d) 3 noise components, (e,f,g) Originalsignal superimposed with different noise components

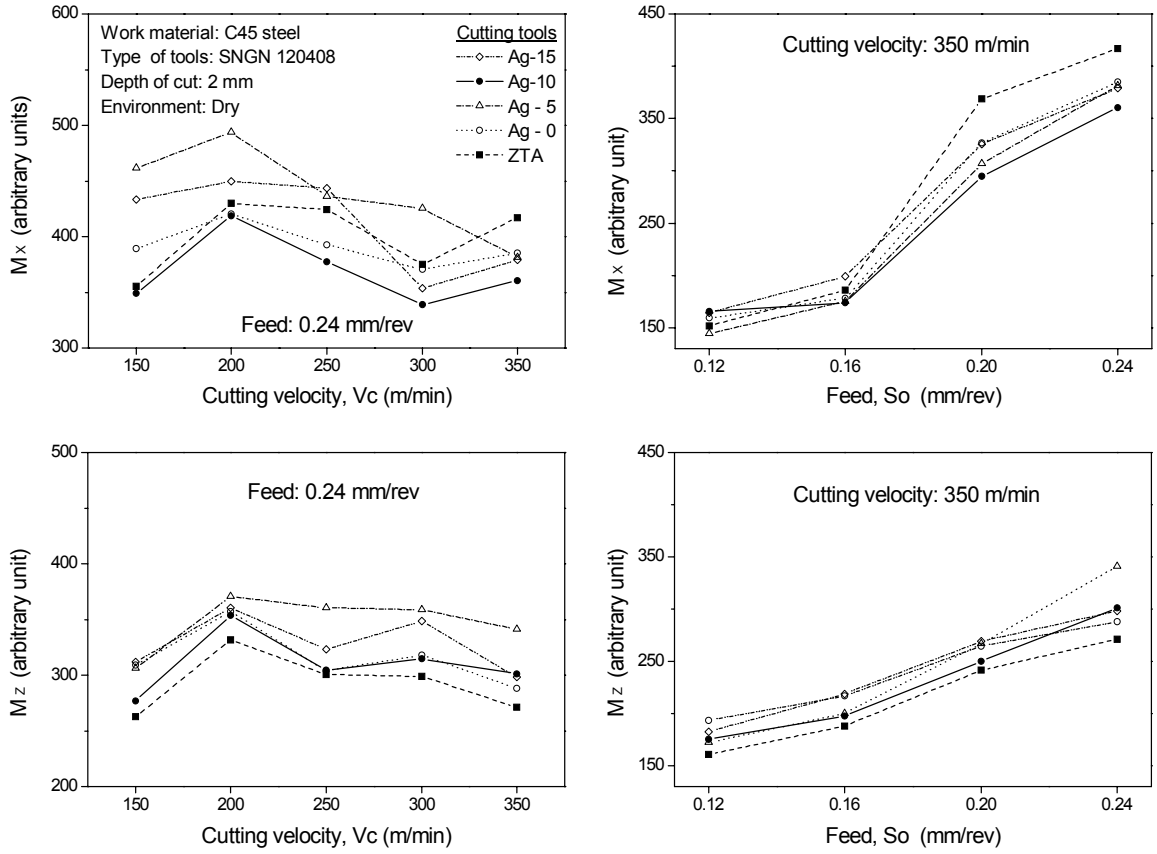

Fig.8. Variation of M_X and M_Z with cutting velocity and feed.